Streamwise localization of traveling wave solutions in channel flow

Joshua Barnett, Daniel R. Gurevich, and Roman O. Grigoriev
School of Physics, Georgia Institute of Technology, Atlanta, Georgia 30332-0430, USA
(Dated: April 3, 2017)

Channel flow of an incompressible fluid at Reynolds numbers above 2400 possesses a number of different spatially localized solutions that approach laminar flow far upstream and downstream. We use one such relative time-periodic solution, which corresponds to a spatially localized version of a Tollmien-Schlichting wave, to illustrate how the upstream and downstream asymptotics can be computed analytically. In particular, we show that for these spanwise uniform states the asymptotics predict the exponential localization that has been observed for numerically computed solutions of several canonical shear flows but never properly understood theoretically.

Due to the development of new computational techniques as well as an increase in computing power, our understanding of fluid flows in the transitional and weakly turbulent regime has improved rather dramatically in the past couple of decades. What started as a numerical exploration of minimal flow units with unphysical (e.g., spatially periodic) boundary conditions [1–3] has eventually yielded a large number of both stable and unstable nontrivial solutions to the Navier-Stokes equation featuring simple temporal dynamics. These solutions have produced significant insight into coherent structures [4, 5] that have been routinely observed in experiments and into the self-sustaining physical processes maintaining turbulence in wall-bounded shear flows [6, 7].

In order to better connect numerical results with experiments, computational domains have steadily increased in both the spanwise and streamwise directions. More recent studies discovered that many spatially-periodic solutions start to localize in the spanwise direction [8, 9], in the streamwise direction [10], or both [11, 12], as the domain size increases. In both cases localization results from subharmonic instability. In particular, spanwise localization generates a discrete set of solutions with different width due to the snaking mechanism [13]. The mechanism that controls streamwise localization is however not entirely clear.

Spatial localization plays a crucial role both in extending results obtained on relatively small computational domains to arbitrarily large physical domains and in understanding how different regions of weakly turbulent flows interact with each other. For instance, while temporal aspects of intermittency in weakly turbulent flows were understood with the help of dynamical systems theory [14] a long time ago, the spatial organization of intermittent flows (e.g., the formation of turbulent bands separated by laminar regions) [15–17] is still an open problem, despite some recent advances [18]. The structure of unstable nonchaotic solutions should help us better understand the dynamics and extent of turbulent bands, spots, and puffs in a variety of shear flows and describe how their size varies with the Reynolds number.

Quite a few of the spatially localized solutions computed numerically have been found to exhibit an exponential localization. Although there is some theoretical support for exponential localization in the streamwise direction [9], there is little understanding of the scaling of the upstream and downstream tails of streamwise-localized solutions, the spatial modulation of these tails, or the mechanism that controls the drift speed of streamwise-localized solutions. The aim of this communication is to show that streamwise asymptotics of several dynamically important classes of spatially localized solutions can be described very accurately by using particular solutions of the Orr-Sommerfeld equation.

We will focus on the flow of an incompressible fluid through a channel with parallel planar walls. It is described by the Navier-Stokes equation which, after nondimensionalization by the channel width, takes the form

$$\partial_t \mathbf{v} + \mathbf{v}\cdot\nabla\mathbf{v} = -\nabla p + Re^{-1}\nabla^2\mathbf{v}, \tag{1}$$

where p is the pressure, x is the streamwise, y is the wall-normal, and z is the spanwise coordinate. The laminar solution satisfying the no-slip boundary conditions for the velocity $\mathbf{v}$ at the walls of the channel ($y = \pm 1$) is known as the plane Poiseuille flow: $\mathbf{v}_0 = [U(y), 0, 0]$, where $U = 1 - y^2$. Linearizing (1) about $\mathbf{v}_0$ yields

$$\partial_t \tilde{\mathbf{v}} + U\partial_x\tilde{\mathbf{v}} + vU'\hat{\mathbf{x}} = -\nabla\tilde{p} + Re^{-1}\nabla^2\tilde{\mathbf{v}}, \tag{2}$$

where $\tilde{\mathbf{v}} = [u, v, w] = \mathbf{v} - \mathbf{v}_0$, $\tilde{p} = p + 2Re^{-1}x$, and the prime denotes the derivative with respect to y. For certain lower branch solutions [19], the streamwise perturbation u dominates in the tail regions, so the asymptotics are controlled by the x component of (2). Moreover, if the terms vU', $-\partial_x\tilde{p}$, and $Re^{-1}\partial_x^2 u$ are neglected, the following simple equation is obtained [11, 19]

$$\partial_t u + U\partial_x u = Re^{-1}(\partial_y^2 u + \partial_z^2 u). \tag{3}$$

In general the spanwise and wall-normal components of the velocity cannot be ignored, so we will use a less restrictive approach. With the help of the incompressibility condition $\nabla\cdot\mathbf{v} = 0$, the linear equation (2) can be manipulated [20] to obtain the Orr-Sommerfeld equation

$$\left(\partial_t + U\partial_x - Re^{-1}\nabla^2\right)\nabla^2 v - U''\partial_x v = 0 \tag{4}$$

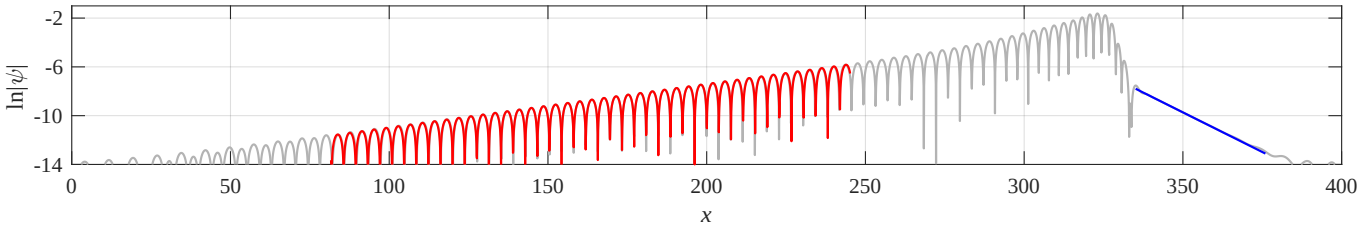

FIG. 1. A snapshot of the magnitude of the stream function ψ describing the MTSW at $Re = 3802$ on the axis $y = 0$ of the channel. Numerical solution is shown in gray, the fits based on the solutions to the Orr-Sommerfeld equation for the leading and trailing tail are shown in blue and red. Numerical accuracy of the solution corresponds to $\ln|\psi| \approx -14$.

for the wall-normal velocity v and the Squires equation

$$\left(\partial_t + U\partial_x - Re^{-1}\nabla^2\right)\eta + U''\partial_z v = 0 \qquad (5)$$

for the wall-normal vorticity $\eta = \partial_z u - \partial_x w$. It is customary to look for solutions to (4) and (5) in the form $v = \hat{v}(y)e^{i\alpha x + i\beta z + \lambda t}$ and $\eta = \hat{\eta}(y)e^{i\alpha x + i\beta z + \lambda t}$, which describe three-dimensional disturbances. In this case $\partial_t[\cdot] = \lambda[\cdot]$, $\nabla^2[\cdot] = (\partial_y^2 - \alpha^2 - \beta^2)[\cdot]$, yielding one-dimensional boundary value problems for $\hat{v}(y)$ and $\hat{\eta}(y)$.

The Orr-Sommerfeld equation (4) can be solved independently; its solution relates the streamwise wavenumber α and spanwise wavenumber β of an infinitesimal disturbance, its transverse profile $\hat{v}(y)$, and the eigenvalue (stability exponent) $\lambda = \sigma + i\omega$. The spectrum of the corresponding boundary value problem is discrete, with infinitely many solutions; we will focus on the one that corresponds to the eigenvalue with the largest real part. Furthermore, since we are primarily interested in streamwise localization, we will only consider two-dimensional (2D) disturbances for which $\beta = 0$, $\eta = 0$, and both wall-normal and streamwise velocity components can be written in terms of a stream function: $u = \partial_y\psi$, $v = -\partial_x\psi$, where $\psi(x, y, t) = \phi(y)e^{i\alpha x + \lambda t}$

Using the Orr-Sommerfeld equation with real α, Orszag [21] has shown that at $Re_c = 5772.22$ the laminar solution becomes unstable toward a spatially periodic modulation with wavenumber $\alpha_c = 1.02056$, and above Re_c the flow becomes turbulent. However, even below Re_c, multiple solutions of (1) have been found, both stable and unstable. One example is nonlinearly saturated 2D Tollmien-Schlichting waves (TSW), which have a spatially uniform envelope. Mellibovsky and Meseguer [10] have recently found a family of 2D localized solutions, termed modulated Tollmien-Schlichting waves (MTSW), related to TSW via a spatial subharmonic instability [22]. TSW correspond to relative equilibria and MTSW to relative periodic orbits: the former become stationary and the latter, temporally periodic in a reference frame moving with some velocity $c > 0$ relative to the walls of the channel. For both types of solutions c is the group velocity. The phase velocity is also equal to c for TSW but is different from c for MTSW.

We have computed MTSW for several different Re on a domain of length $L_x = 400$ (with periodic boundary conditions in the x direction) using the package *Channelflow* [23]. The stream function associated with one such solution at $Re = 3802$ is shown in Figs. 1 and 3(a). A distinguishing feature of all MTSW is that their localization is exponential, both in the upstream and in the downstream direction, with the solution approaching a laminar profile $\mathbf{v}_0$ for $x \to \pm\infty$. This localization can also be understood using the Orr-Sommerfeld equation.

Unlike the stability analysis, we should look at disturbances with a streamwise wavenumber that is complex, $\alpha = q + is$, where the real part q describes the spatial modulation and the imaginary part s, the spatial attenuation of the tails of a localized solution. Let $\xi = x - ct$ describe the streamwise coordinate in the reference frame moving with speed c (i.e., the group velocity of the MTSW), such that, for $\xi \to \pm\infty$, the tails of the solution can be written in the form $\psi(\xi, y, t) = \phi(y)e^{iq\xi - s\xi}e^{\sigma' t}e^{i\omega' t}$. Since the MTSW is temporally periodic in this reference frame, we should have

$$\begin{aligned} \sigma' &\equiv \sigma(q, s) - cs = 0, \\ \omega' &\equiv \omega(q, s) + cq = \frac{2\pi}{T}n, \end{aligned} \qquad (6)$$

where T is the temporal period of the MTSW and n is an integer. The system of equations (6) can be solved with the help of the Matlab package *chebfun* [24] and possesses several solutions for the relevant range of Reynolds numbers. Those with $s > 0$ describe the downstream/leading tail ($\psi \to 0$ for $\xi \to \infty$) and those with $s < 0$, the upstream/trailing tail ($\psi \to 0$ for $\xi \to -\infty$). Note that the leading mode of (4) may not satisfy conditions (6) for either positive or negative s for any q and n. In this case the next leading mode has to be considered, etc.

When $q = 0$ the second equation in (6) is satisfied identically for $n = 0$, so only the first equation needs to be solved for s. There are typically two solutions, one with positive and one with negative s (see Fig. 2). In particular, for $Re = 3802$ we find two solutions $\mathbf{a} = (q, s, n)$ with $q = 0$ and one with $q \neq 0$: $\mathbf{a}_1 = (0, 0.130, 0)$, $\mathbf{a}_2 = (0.826, -0.0354, 1)$, and $\mathbf{a}_3 = (0, -0.00642, 0)$. The first two accurately describe, respectively, the leading and the trailing tail of the corresponding MTSW, as Fig.

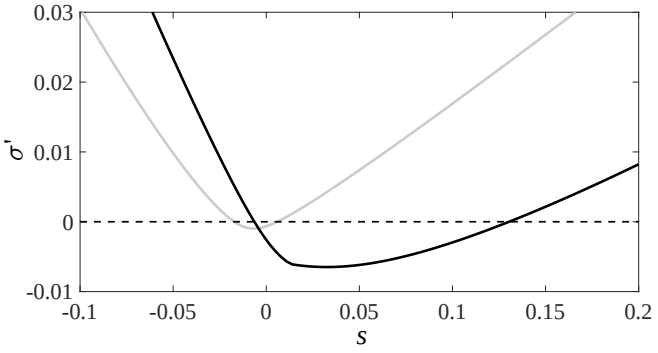

FIG. 2. The growth rate in the co-moving frame, computed using the Orr-Sommerfeld equation (4) (black line) and the approximate equation (3) (gray line) for $q = 0$ and $Re = 3802$.

1 illustrates. The best fit values found using the fully nonlinear numerical solution [$\mathbf{a}_1^{\rm num} = (0, 0.129, 0)$ for the leading tail and $\mathbf{a}_2^{\rm num} = (0.826, -0.0355, 1)$ for the trailing tail] are in excellent agreement with predictions based on the Orr-Sommerfeld equation. On the other hand, (3) predicts incorrect asymptotics for both tails. This is expected since for the MTSW, u and v are comparable.

We can further confirm the accuracy of the predictions based on linearization by comparing the spatial profiles of the stream function computed using the full Navier-Stokes equation (1) and the Orr-Sommerfeld equation (4). The results are compared in Fig. 3(b) for the leading tail and in Fig. 3(c) for the trailing tail. In both cases we again find excellent agreement.

The structure of the tails has an interesting physical interpretation. In the stationary reference frame, the leading tail describes a disturbance $\psi \propto \phi_1(y)e^{i\alpha_1 x+\lambda_1 t}$ about the laminar flow profile that is unstable ($\sigma > 0$), vanishes at $x \to \infty$ ($s > 0$), and has no spatial ($q = 0$) or temporal ($\omega = 0$) modulation. The transverse profile of this disturbance (cf. Fig. 3(b)) corresponds to a monotonic increase in the shear rate of the flow in the central region $|y| < 0.45$ of the channel. This increase in the shear can be thought of as promoting the Kelvin-Helmholtz instability, which, unlike the initial disturbance, has an oscillatory character. The core of the MTSW (which we define as the region shown in Fig. 3(a), where $|\psi|$ and the velocity perturbation are the largest) can therefore be thought of as a result of nonlinear saturation in the spatial and temporal modulation.

Eventually the perturbation starts to decay back to the laminar state. This decay is controlled by the two solutions of the Orr-Sommerfeld equation with $s < 0$ and $\sigma < 0$. Hence, in general, one might expect to see a linear combination of these two solutions

$$\psi = A_2\phi_2(y)e^{i\alpha_2 x+\lambda_2 t} + A_3\phi_3(y)e^{i\alpha_3 x+\lambda_3 t} \qquad (7)$$

with the coefficients A_2 and A_3 determined by the boundary conditions in the region where the trailing tail is matched to the core region. Since the temporal dynamics in the core region are dominated by nearly harmonic modulation with frequency $2\pi/T$, it is natural to expect the mode with $n = 1$ to dominate over the mode with $n = 0$ (i.e., $|A_2| \gg |A_3|$), so the second term in (7) can be neglected. This is indeed what we find: the first term alone describes both the streamwise profile of the trailing tail of the numerical solution (cf. Fig. 1) and its wall-normal profile (cf. Fig. 3(c)).

If we fix t and vary x (or fix x and vary t), the MTSW becomes a homoclinic orbit that starts and ends at the laminar state (cf. Fig. 4(a)). The leading tail (aligned along the Z axis in this projection) describes the transition from laminar flow to the neighborhood of a corresponding upper branch TSW shown in Fig. 4(b). Since this TSW is itself unstable on a long domain [22], the orbit eventually leaves its neighborhood and spirals back toward the laminar solution, bypassing the lower branch TSW. This final piece of the orbit corresponds to the trailing tail.

The group velocity c has been computed simultaneously with MTSWs using a matrix-free Newton-Krylov method [25]. It is natural to ask whether c can instead be found from linearization. Front propagation theory predicts that, for a pulled front, the front speed and streamwise wavenumber are uniquely defined by a solution to the following system of equations [26]:

$$c = i\frac{\partial\lambda}{\partial\alpha} = \frac{\mathrm{Re}(\lambda)}{\mathrm{Im}(\alpha)}, \qquad (8)$$

which, in particular, requires $\partial\sigma/\partial s = \sigma/s$. For channel flow, this equation has no solutions for $q = 0$ in the range of Re we explored, so the speed of the MTSW is not selected by a linear mechanism (i.e., the leading tail corresponds to a pushed front). Therefore, the speed of MTSW is controlled by the core region, rather than the leading tail, and hence the drift speed should be different for different localized solutions. Furthermore, since the first of the equalities in (8) does not hold, neither does the conventional relationship $c = -\partial\omega/\partial q$ for the group velocity. Indeed, the system (6) has a discrete set of solutions, so the variation of the temporal frequency with spatial wavenumber is meaningless.

It has been noticed previously that the leading and the trailing tail of streamwise-localized solutions of shear flows decay spatially at different rates. In particular, for doubly-localized solutions of channel flow, it was found that the leading tail decays at a rate that is approximately constant, while the trailing tail decays at a rate $|s| \propto Re^{-1}$ [12]. We find that the general trends are similar for MTSW which lack spanwise localization: the decay rate s_1 for the leading tail increases weakly with Re (cf. Fig. 5(a)), while the decay rate for the trailing tail decreases as a power law $|s_2| \propto Re^{\gamma}$ with the exponent $\gamma = -1.75$. In both cases the localization is the strongest at smaller Re and solutions gradually de-localize as Re

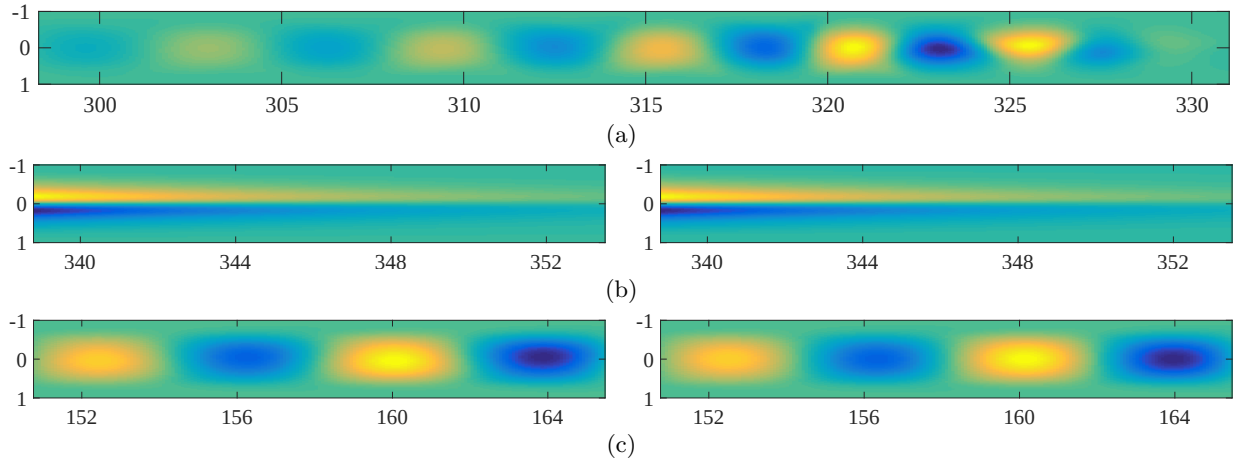

FIG. 3. The stream function ψ describing the MTSW at $Re = 3802$: (a) the core region, (b) a segment of the leading edge, (c) a segment of the trailing edge. In (b) and (c) numerical solution is on the left, analytical solution is on the right, and the stream function scale is arbitrary. The horizontal and vertical axes correspond to x and y, respectively, with the x coordinate corresponding to that in Fig. 1. The colormap corresponding to (a) is shown in Fig. 4(b).

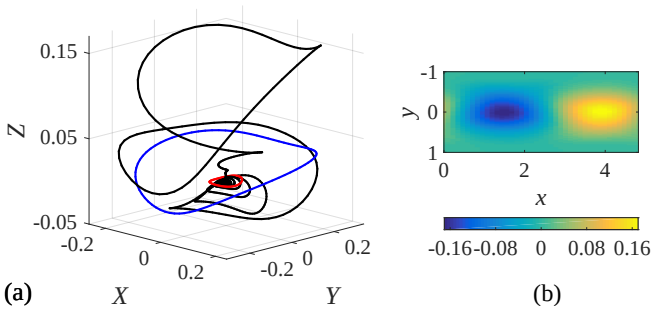

FIG. 4. (a) The homoclinic orbit. MTSW and the corresponding upper and lower branch TSW [10] are shown as black, blue, and red curves, respectively. The coordinates are $X = v$, $Y = \partial_x v$, and $Z = u$ at $y = 0$ and t-fixed, with the origin corresponding to laminar flow. (b) The stream function ψ for the upper branch TSW.

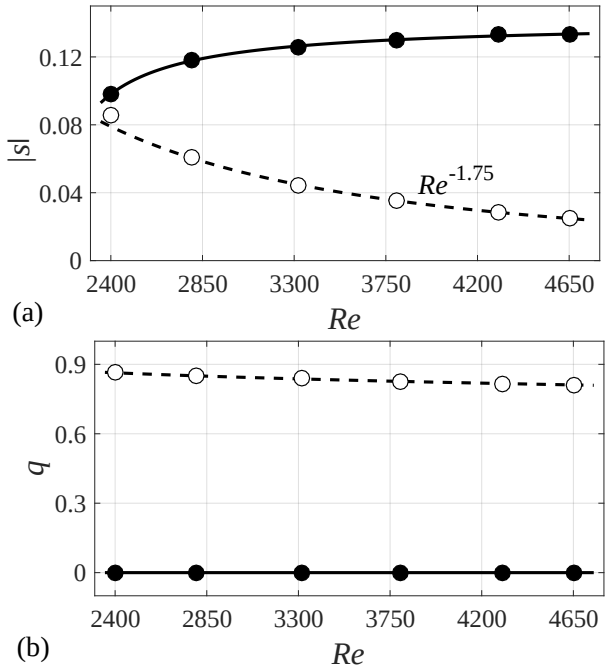

FIG. 5. The spatial decay rate $|s|$ (a) and the wavenumber q (b) of the tails of MTSW. The data for the leading (trailing) tail are shown as filled (open) symbols. MTSW is stable for $Re \leq 3802$ and unstable for $Re \geq 4300$.

increases. The general agreement suggests that the description presented here should apply in equal measure to solutions that have both streamwise and spanwise localization, although the specific results would depend on the properties of a particular solution. For instance, for MTSW, the leading tail does not have spatial modulation and the trailing tail does (cf. Fig. 5(b)), while for the doubly-localized solution the opposite is true.

To conclude, we have demonstrated that the asymptotics of streamwise-localized 2D modulated Tollmien-Schlichting waves in channel flow are well-described by solutions to the Orr-Sommerfeld equation with a complex streamwise wavenumber. This approach is capable of describing both the streamwise and spanwise asymptotics of localized solutions for any flow profile $U(y)$, provided that they are described by either relative equilibria or relative periodic orbits, regardless of their stability. Spanwise localization can be described using solutions of the Orr-Sommerfeld equation with real α and complex $\beta \neq 0$ as shown previously for relative equilibria in plane Couette flow [9]. For doubly localized solutions, all components of the velocity are nonzero [12], so, in addition to the Orr-Sommerfeld equation (4), one also has to solve the Squire equation (5) for complex α and β. The streamwise and spanwise velocity components can then

be computed by solving additional equations

$$(\partial_x^2 + \partial_z^2)u = \partial_z\eta - \partial_x\partial_y v,$$
$$(\partial_x^2 + \partial_z^2)w = -\partial_x\eta - \partial_y\partial_z v. \quad (9)$$

Due to its linearity, the Orr-Sommerfeld equation is dramatically easier to study analytically compared with the Navier-Stokes equation. Until recently, the fully nonlinear solutions of Navier-Stokes could be computed and studied only numerically. The results presented here and in related studies [9, 11, 12, 19] give us hope that we can understand some of their properties analytically. In particular, we found that the group velocity of localized solutions is controlled by a nonlinear mechanism and hence is not universal, which has important implications for the structure and dynamics of turbulent bands, spots, and puffs in various intermittent flows.

This work was supported in part by the National Science Foundation under Grant No. CMMI-1234436. We are grateful to F. Mellibovsky and A. Meseguer for sharing some of the localized solutions they have computed and to J. Gibson for sharing his numerical code *Channelflow* and for helping us set up the simulations.

[1] M. Nagata, J. Fluid Mech **217**, 519 (1990).
[2] G. Kawahara and S. Kida, J. Fluid Mech. **449**, 291 (2001).
[3] F. Waleffe, J. Fluid Mech. **435**, 93 (2001).
[4] A. K. M. F. Hussain, Phys. Fluids **26**, 2816 (1983).
[5] L. Sirovich, Quart. Appl. Math. **45**, 561 (1987).
[6] F. Waleffe, Phys. Fluids **9**, 883 (1997).
[7] J. Wang, J. Gibson, and F. Waleffe, Phys. Rev. Lett **98**, 204501 (2007).
[8] T. M. Schneider, J. F. Gibson, and J. Burke, Phys. Rev. Lett **104**, 104501 (2010).
[9] J. F. Gibson and E. Brand, J. Fluid Mech. **745**, 25 (2014).
[10] F. Mellibovsky and A. Meseguer, J. Fluid Mech. **779**, R1 (2015).
[11] E. Brand and J. F. Gibson, J. Fluid Mech. **750**, R3 (2014).
[12] S. Zammert and B. Eckhardt, J. Fluid Mech. **761**, 348 (2014).
[13] J. Burke and E. Knobloch, Chaos **17**, 037102 (2007).
[14] Y. Pomeau and P. Manneville, Comm. Math. Phys. **74**, 189 (1980).
[15] I. J. Wygnanski and F. H. Champagne, J. Fluid Mech. **59**, 281 (1973).
[16] D. Barkley and L. S. Tuckerman, Phys. Rev. Lett. **94**, 014502 (2005).
[17] A. Meseguer, F. Mellibovsky, M. Avila, and F. Marques, Phys. Rev. E **80**, 046315 (2009).
[18] M. Chantry, L. S. Tuckerman, and D. Barkley, J. Fluid M. **791**, R8 (2016).
[19] S. Zammert and B. Eckhardt, Phys. Rev. E **94**, 041101 (2016).
[20] P. J. Schmid and D. S. Henningson, *Stability and Transition in Shear Flows*, Vol. 142 (Springer Science & Business Media, Berlin, 2012).
[21] S. A. Orszag, J. Fluid Mech. **49**, 75 (1971).
[22] A. Drissi, M. Net, and I. Mercader, Phys. Rev. E **60**, 1781 (1999).
[23] J. F. Gibson, "Channelflow: A spectral Navier-Stokes simulator in C++," (2012), `channelflow.org`.
[24] T. A. Driscoll, N. Hale, and L. N. Trefethen, "Chebfun guide," (2014), `www.chebfun.org`.
[25] F. Waleffe, Phys. Rev. Lett. **81**, 4140 (1998).
[26] W. van Saarloos, Phys. Rev. A **39**, 6367 (1989).